Int. J. Solids Structures, 1972, Vol. 8, pp. 1319 to 1338. Pergamon Press. Printed in Great Britain

DETERMINATION OF ELASTIC STRESSES AT NOTCHES AND CORNERS BY INTEGRAL EQUATIONS

MARTIN R. BARONE

General Motors Applied Research Center, Warren, Michigan

and

ARTHUR R. ROBINSON

Department of Civil Engineering, University of Illinois at Urbana-Champaign, Urbana, Illinois

Abstract—An integral equation method is presented which permits evaluation of stress and displacement fields in two-dimensional elastic solids near corners and notches. The procedure begins by using well known expressions of an asymptotic character for the fields near the points in question. Unknown coefficients, one of which will be a stress intensity factor in the case of a cracked plate, are treated as generalized displacements. Suitable test solutions are developed to express the generalized displacements in terms of integrals involving far-field quantities. Sample numerical solutions are presented for notched and cracked plates.

INTRODUCTION

IN THIS paper an effective numerical method for determining stress near corners and notches in finite two-dimensional bodies is presented. It is assumed that the material is linearly elastic and that the displacements are small.

As is well known, the formulation of the problem in accordance with the small displacement theory may give rise to stress singularities. Obviously, this is an idealization of the physical problem in which yielding or other nonlinear behavior precludes the possibility of infinite stresses. Nevertheless, the determination of singular elastic stress states is an important consideration in problems where small scale yielding is encountered [1].

A variety of exact singular solutions for infinite regions are readily available [2, 3]. However, the problem of obtaining an exact solution in a bounded region with prescribed boundary values is generally intractable. One is therefore usually compelled to seek approximate schemes which are capable of providing satisfactory results with a reasonable expenditure of computational effort.

The most commonly used numerical methods for solving boundary value problems with stress singularities have been based on boundary collocation and finite element techniques. Recently, however, the work of Rizzo *et al.* [4, 5] has revived interest in the singular integral equations of classical elastostatics, via the direct (real variable) potential approach. Cruse and Vanburen [6] have applied the direct potential method to a thick plate with an edge crack in order to determine the nonanalytic stress distribution. A somewhat different path was followed by Bueckner [7] and Tirosh [8] who established singular integral equations, in complex form, for two-dimensional crack problems.

Although both these expressions include the character of the singularity, they appear to lack the generality and conceptual simplicity of the integral equations generated directly in terms of the real variable potentials cited earlier.

The proposed formulation is an extension of the direct potential method in that the character of the stress singularity enters the resulting singular integral equations explicitly. In the formulation the asymptotic character of the nonanalytic stress state is expressed by an eigenfunction expansion where each of the eigenfunctions is known to within a multiplicative constant. These constants serve as generalized displacements. The kernels for the integral equations corresponding to points along smooth portions of the boundary are obtained from solutions to concentrated force problems in the usual manner. However, new kernels are derived in the formulation of the integral equations at the points associated with stress singularities. The two types of integral equations form a coupled system involving the generalized displacements and boundary values as unknowns.

The main advantage of the proposed method is that it leads to a well conditioned system of linear algebraic equations for bodies of almost any shape. In addition, it turns out that the generalized displacements at a singular point depend almost entirely on the boundary values at fairly remote points. This appears to have a stabilizing effect on the solution.

As will be seen later, the integral equations developed in the present study which determine the character of the stress singularities involve only the far-field displacements. In contrast, Bueckner's integral equation extends over an area near the singularity [7]. Tirosh [8] arrives at an integral equation for an antiplane case in which a stress intensity factor is determined directly in terms of far-field quantities.

INTEGRAL EQUATIONS AT REGULAR AND IRREGULAR BOUNDARY POINTS

The integral equations are formulated for an elastic two-dimensional region enclosed by a curve, the boundary. A point on the boundary is regular if the tangent at the point is continuously turning. A point at which the tangent is not uniquely defined is termed irregular. The tip of a crack or the vertex of a wedge are particular examples of irregular boundary points.

The integral equation formulation for regions with irregular boundary points is based on Betti's reciprocal theorem.† The success of this approach, as in classical potential theory, depends entirely on the judicious choice of the "test" solutions, commonly referred to as auxiliary solutions. A suitable choice of the auxiliary solutions makes it possible to express the unknown displacements at a boundary point P in terms of work integrals that contain the boundary displacements and tractions associated with the actual solution sought. The resulting integral equations will depend in form on whether the boundary point is regular or irregular. A detailed development of the integral equations at irregular points will be presented in the following sections. First, however, it is helpful to summarize the development of the well known integral equation technique for regular points [4] in order to motivate the subsequent extension to an irregular point.

Integral equations at regular boundary points

Consider a two-dimensional region $D+L$, where D signifies the open region and L the bounding contour. The actual field parameters are denoted by

$$t_j(Q);\ \text{tractions}$$

† This method was first applied to elasticity problems by the Italian school of elasticians (see Love [9]) in the last century.

$$u_j(p);\ \text{displacements}$$

$$\sigma_{ij}(p);\ \text{stresses}$$

where p is a point in $D+L$ and Q is a boundary point. The indices $(i = 1, 2)$ and $(j = 1, 2)$ refer to the (x, y) coordinate directions.

In the case of the two-dimensional problem, the auxiliary system is derived from the well-known Kelvin solutions associated with the concentrated forces F_1 and F_2 acting in the x and y directions, respectively.

The tractions and displacements at some boundary point, Q, due to the ith concentrated force at a point P are denoted by

$$t_{ij}^*(Q);\ \text{tractions}$$

$$u_{ij}^*(Q);\ \text{displacements}$$

where $j\,(j = 1, 2)$ refers to the x and y directions.

Since the auxiliary solution is unbounded at P, a small region which contains P is removed from the body before the reciprocal theorem is applied. The excluded region, D_ε, is conveniently taken as a circle centered at P with a radius ε.

If the actual displacements and tractions, which are regular at P, are expanded about P in a Taylor series, it can be readily seen that the reciprocal relation for $\varepsilon \to 0$ can be expressed as

$$\alpha_{ij}u_j(P) + \int_L t_{ij}^*(Q)u_j(Q)\,\mathrm{d}s(Q) = \int_L t_j(Q)u_{ij}^*(Q)\,\mathrm{d}s(Q) \tag{1}$$

where

$$\alpha_{ij} = 0 \quad \text{if} \quad i \neq j.$$

It follows from equation (1) that the Kelvin auxiliary forces $(\alpha_{11} = F_1,\ \alpha_{22} = F_2)$ acting at P in effect "pick out" the actual displacements at P.

Integral equations at irregular boundary points

In order to develop the proposed method it is first necessary to establish the form of the displacements in the vicinity of a notch. These displacements, expressed in polar coordinates, take the form [10, 11] (Fig. 8)

$$\begin{aligned} U_\rho &= \rho^\lambda A(\phi) \\ U_\phi &= \rho^\lambda B(\phi) \end{aligned} \tag{2}$$

where λ is a constant. By virtue of equations (2) the two-dimensional equilibrium equations can be reduced to†

$$\begin{aligned} &\frac{\mathrm{d}^2A(\phi)}{\mathrm{d}\phi^2} + \frac{\lambda-3+4\nu}{1-2\nu}\frac{\mathrm{d}B(\phi)}{\mathrm{d}\phi} + \frac{2(1-\nu)}{1-2\nu}(\lambda^2-1)A(\phi) = 0 \\ &\frac{2(1-\nu)}{1-2\nu}\frac{\mathrm{d}^2B(\phi)}{\mathrm{d}\phi^2} + \frac{\lambda+3-4\nu}{1-2\nu}\frac{\mathrm{d}A(\phi)}{\mathrm{d}\phi} + (\lambda^2-1)B(\phi) = 0. \end{aligned} \tag{3}$$

General expressions for $A(\phi)$ and $B(\phi)$ can be obtained from equations (3) in the usual manner. The stipulation that the solution satisfy certain prescribed homogeneous boundary

† These equations are required in the Appendix.

conditions along the sides of the notch leads to a characteristic equation which is a function of λ and the notch angle. It turns out that there are an infinite number of eigenvalues (λ_m; $m = 1, 2, \ldots$) which satisfy this equation and that each of the corresponding eigenfunctions can be determined to within a multiplicative constant. The displacements near an irregular boundary point can then be expressed as an eigenfunction expansion.

In general the eigenvalues (λ_m; $m = 1, 2, \ldots$) are complex. It is possible, without loss of generality, to regard λ_m as real in the following development. Under the assumption that the λ_m are real, the displacement and stress fields can be written as

(a) *The actual displacement field.*

$$\begin{aligned} U_\rho &= \sum_m D_{\rho m} \\ U_\phi &= \sum_m D_{\phi m}. \end{aligned} \tag{4}$$

(b) *The actual stress field.*

$$\begin{aligned} S_\rho &= \sum_m T_{\rho m} \\ S_\phi &= \sum_m T_{\phi m} \\ S_{\rho\phi} &= \sum_m T_{\rho\phi m}. \end{aligned} \tag{5}$$

The mth term of each of these expansions is given by:

(a) *The mth displacement field.*

$$\begin{aligned} D_{\rho m} &= K_m A_m(\phi)\rho^{\lambda_m} \\ D_{\phi m} &= K_m B_m(\phi)\rho^{\lambda_m}. \end{aligned} \tag{6}$$

(b) *The mth stress field.*

$$\begin{aligned} T_{\rho m} &= K_m P_m(\phi)\rho^{\lambda_m - 1} \\ T_{\phi m} &= K_m Q_m(\phi)\rho^{\lambda_m - 1} \\ T_{\rho\phi m} &= K_m R_m(\phi)\rho^{\lambda_m - 1} \end{aligned} \tag{7}$$

where the unknown constants K_m are generalized displacements. The functions $A_m(\phi), \ldots, R_m(\phi)$ in the above equations are defined by the following relations

$$\begin{aligned} A_m(\phi) &= C_{jm} a_j(\phi, \lambda_m) \\ B_m(\phi) &= C_{jm} b_j(\phi, \lambda_m) \\ P_m(\phi) &= C_{jm} p_j(\phi, \lambda_m) \\ Q_m(\phi) &= C_{jm} q_j(\phi, \lambda_m) \\ R_m(\phi) &= C_{jm} r_j(\phi, \lambda_m) \end{aligned} \tag{8}$$

where $j = 1, 2, 3, 4$. The $a_j(\phi, \lambda_m)$ through $r_j(\phi, \lambda_m)$ are trigonometric functions and the constants C_{jm} are eigenvectors determined from the homogeneous boundary conditions (12).

The most important step in the treatment of boundary value problems where some of the boundary points are irregular is to establish equations that relate the generalized

displacements to the displacements and traction along the boundary. The possibility of establishing these relations in a manner similar in principle to the approach taken in the formulation of the integral equations at a regular point suggests itself if one recognizes the analogy between the displacements (u_1, u_2) at a regular point and the generalized displacements at an irregular point. Since the Kelvin auxiliaries pick out the corresponding displacements (u_1, u_2), it is reasonable to inquire whether certain auxiliary solutions can be found which pick out the corresponding generalized displacements. It turns out that such auxiliary solutions do exist.

A question which arises naturally at this point is: what must be the form of the auxiliary solution which picks out the nth generalized displacement? It suffices, in answering this question, to refer to the form of the actual displacements as given by equations (6) and to observe that the reciprocal relation would involve work terms such as the auxiliary tractions multiplied by the corresponding terms of the actual displacements along a small circular arc of radius ε which excludes the irregular point from the body (see Fig. 1) Clearly, the auxiliary solution must be chosen so that the work terms remain bounded as ε approaches zero. If such a set of solutions exists, then we are led to the conclusion that they are of the same form as the corresponding nth term of the actual solution and that the characteristic exponent λ_n^* is the negative of the associated characteristic exponent λ_n. That is,

(a) *The nth auxiliary displacements.*

$$\begin{aligned} D_{\rho n}^* &= K_n^* A_n^*(\phi)\rho^{\lambda_n^*} \\ D_{\phi n}^* &= K_n^* B_n^*(\phi)\rho^{\lambda_n^*}. \end{aligned} \tag{9}$$

(b) *The nth auxiliary stresses.*

$$\begin{aligned} T_{\rho n}^* &= K_n^* P_n^*(\phi)\rho^{\lambda_n^*-1} \\ T_{\phi n}^* &= K_n^* Q_n^*(\phi)\rho^{\lambda_n^*-1} \\ T_{\rho\phi n}^* &= K_n^* R_n^*(\phi)\rho^{\lambda_n^*-1} \end{aligned} \tag{10}$$

where $\lambda_n^* = -\lambda_n$ and K_n^* are suitably chosen constants. The functions $A_n^*(\phi), \ldots, R_n^*(\phi)$ are obtained by replacing λ_n by $-\lambda_n$ in the corresponding functions associated with actual solution [see equations (8)].

These auxiliary solutions possess a remarkable property; they satisfy the same boundary conditions on the faces of the notch as the original solution.

The preceding heuristic arguments that led to the formulation of the auxiliary solutions require verification. This can be accomplished most directly and without loss of generality by considering the manner in which the reciprocal theorem relates the actual solution and the nth auxiliary solution in the specific case of a cracked plate subjected to prescribed tractions as shown in Fig. 1. Since the crack is traction-free, the tractions associated with each component of the actual solution must vanish. This condition can be expressed in terms of the characteristic equation which for the traction-free crack becomes

$$\sin^2 2\lambda\pi = 0 \tag{11}$$

where

$$\lambda_m = \frac{m}{2}; \qquad (m = 1, 2, 3, \ldots).$$

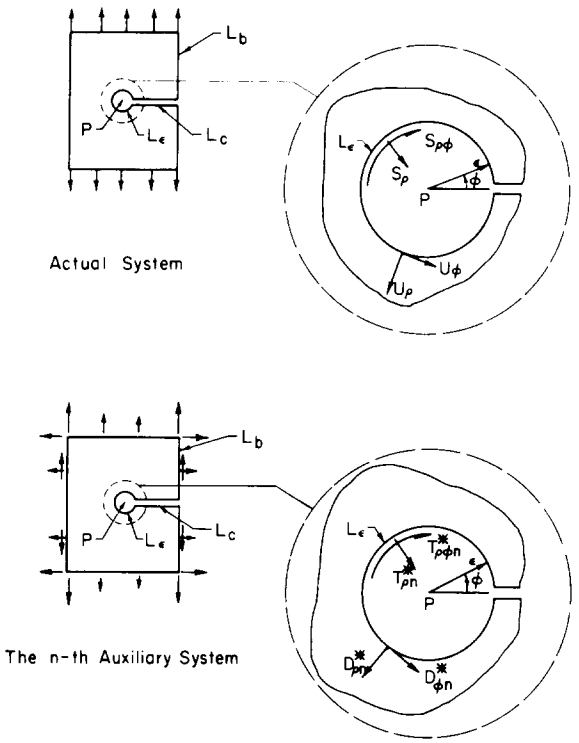

FIG. 1. Actual and auxiliary systems for a cracked plate.

These eigenvalues are positive and therefore conform to the physical requirement that the displacements remain bounded and continuous at the irregular point, i.e. the crack tip. Obviously, the auxiliary displacements need not satisfy this requirement.

This reciprocal work terms are evaluated along the circular arc L_ε (Fig. 1) of radius ε and along the remainder of the boundary. For the present it suffices to introduce only the work terms along the circular arc L_ε and the crack boundary L_c. Let:

w_{12} = The work of the actual tractions through the nth auxiliary displacements along $L_\varepsilon + L_c$.

w_{21} = The work of the nth auxiliary tractions through the actual displacements along $L_\varepsilon + L_c$.

The difference of these terms is expressed as

$$w_d = w_{12} - w_{21} = \sum_m K_m \Gamma_{mn} \varepsilon^{\lambda_m + \lambda_n^*} + \Delta(\varepsilon) \tag{12}$$

where K_m are generalized displacements and $\Delta(\varepsilon)$ is the reciprocal work difference along L_c. The term Γ_{mn} is the work difference along L_ε and is given by:

$$\Gamma_{mn} = -K_n^* \int_0^{2\pi} [[P_m(\phi)A_n^*(\phi) - P_n^*(\phi)A_m(\phi)] + [R_m(\phi)B_n^*(\phi) - R_n^*(\phi)B_m(\phi)]]\varepsilon \, d\phi \tag{13}$$

where K_n^* is a suitably chosen constant. The reciprocal theorem relates w_d to bounded integrals evaluated along the remaining portion of the boundary L_b. Therefore, if w_d is to have a meaningful interpretation, λ_n^* must be chosen so that

$$\lim_{\varepsilon \to 0} w_d$$

is bounded for all m and n. In addition,

$$\lim_{\varepsilon \to 0} \sum_m K_m \Gamma_{mn} \varepsilon^{\lambda_m + \lambda_n^*}$$

must be nonzero for at least one m. If the exponent λ_n^* is chosen so that

$$\lambda_n^* = -\lambda_n$$

the above requirements are satisfied. Furthermore, since λ_n is a solution of equation (11), λ_n^* or $-\lambda_n$ is also a solution. Consequently, each auxiliary solution satisfies the traction-free boundary conditions and $\Delta(\varepsilon)$ is identically zero. Although this argument is presented with reference to the traction-free crack the resulting conclusion can be generalized in terms of the following proposition:

Proposition 1. If each component of the actual solution satisfies a set of homogeneous boundary conditions, then there exists a corresponding auxiliary solution with $\lambda_n^* = -\lambda_n$ satisfying the boundary conditions.

There is one more remarkable property associated with the auxiliary solutions which also applies in the general case.

Proposition 2. The nth auxiliary solution picks out only the corresponding nth generalized displacement.

The proofs of these propositions are developed in the Appendix.

The general form of the integral equations at irregular boundary points must be developed by considering a general situation, not a free crack. For the wedge, complex eigenvalues occur in general, sometimes even for the most singular solutions, as in the fixed-free case where the wedge opening angle is π. In the simpler case where the eigenvalues are real, there is one solution associated with each eigenvalue [see equation (6)]. When the eigenvalues are complex there are two independent solutions for each complex conjugate pair of eigenvalues. These independent solutions are constructed from the real and imaginary parts of equation (6). The corresponding auxiliary solutions are obtained from equation (9) in a similar fashion. For any given region, Fig. 2, the boundary tractions and displacements associated with the actual and auxiliary solutions will now be denoted by

$t_j(Q)$; actual tractions

$u_j(Q)$; actual displacements

$t_{ij}^*(Q)$; auxiliary tractions

$u_{ij}^*(Q)$; auxiliary displacements

where j ($j = 1, 2$) indicates the (x, y) coordinate directions and i ($i = 1, 2$) refers to the two independent real auxiliary solutions which are derived from the corresponding nth complex solutions [10].

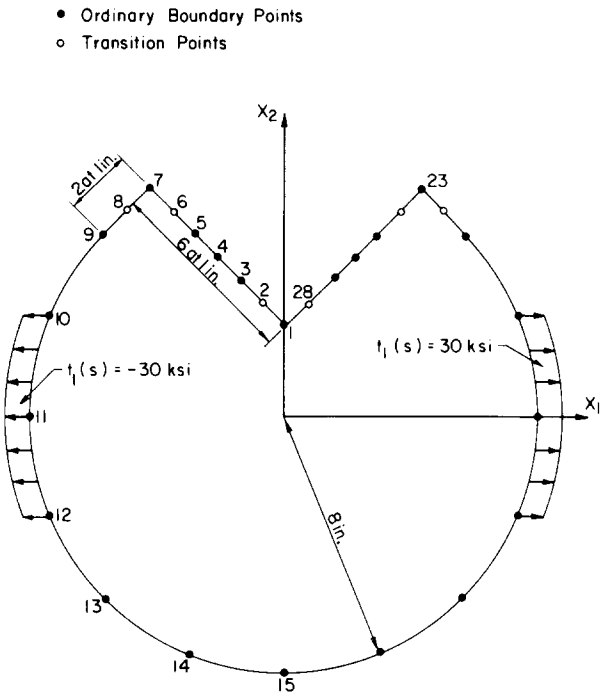

FIG. 2. Notched circular plate subjected to prescribed tractions.

Before the reciprocal theorem is applied to the actual and auxiliary solutions a small circular sector D_ε which contains the irregular point is removed from $D+L$. The reciprocity relations for $D+L-D_\varepsilon$ are

$$-\int_{L_\varepsilon}[t_j(Q_\varepsilon)u_{ij}^*(Q_\varepsilon)-t_{ij}^*(Q_\varepsilon)u_j(Q_\varepsilon)]\,ds(Q_\varepsilon) = \int_{L-L_\varepsilon}[t_j(Q)u_{ij}^*(Q)-t_{ij}^*(Q)u_j(Q)]\,ds(Q). \tag{14}$$

Equations (14) can be recast by noting that for a sufficiently small ε the actual solution can be expressed in terms of an eigenfunction expansion. Further simplification results after the integrand on the left side of equation (14) is expressed in terms of the polar coordinates (ε, ϕ). It can then be seen that the work done over the arc L_ε does not depend on ε. Therefore, letting ε approach zero in equation (14) gives

$$\sum_{l=1}^{2} K_n^{(l)}\Gamma_{ni}^{(l)} = \int_L [t_j(Q)U_{ij}^*(Q)-t_{ij}^*(Q)U_j(Q)\,ds(Q)] \tag{15}$$

where the $K_n^{(l)}$ are the two independent generalized displacements associated with the real and imaginary parts of the nth actual displacement field. The $\Gamma_{ni}^{(l)}$ serve as generalized forces.

SPECIAL CONSIDERATIONS

Rigid body displacements at irregular boundary points

The integral equation formulation for the rigid body rotation at an irregular boundary point follows directly from the formal development of the preceding section. Equations (9) and (10) with $\lambda_n = -1$ provide the fundamental rotational auxiliary solution which, according to Proposition 1, satisfies the homogeneous boundary conditions.

In the case of the rigid body translations, the integral equations are derived with the aid of the Kelvin solutions and take on the same form as the integral equations (1) at regular boundary points. The only difference is that the α_{ij} at irregular points need not be zero for i unequal to j.

Crack problems

One can easily see that the Kelvin auxiliary solutions lead to an indeterminate integral equation formulation at points along a crack by noting that these solutions pick out only two independent combinations of the four displacements (two on each side of the crack):

$$\alpha_{ij}[u_j(P_1)+u_j(P_2)]+\int_L t_{ij}^*(Q)u_j(Q)\,ds(Q)$$

$$=\int_L t_j(Q)u_{ij}^*(Q)\,ds(Q) \tag{16}$$

where $\alpha_{ij}=0$ for $i\neq j$ and where the coincident but physically distinct points P_1 and P_2 are associated with opposite sides of the crack. Since equations (16) contain the sum of the displacements at P_1 and P_2, we seek auxiliary solutions that pick out the difference of the displacements at P_1 and P_2. Such solutions are readily available [3] and correspond to equal and opposite prying forces acting at some point along a semi-infinite crack in an infinite body. Using these solutions as auxiliaries, we find

$$\beta_{ij}[u_j(P_1)-u_j(P_2)]+\int_L t_{ij}^*(Q)u_j(Q)\,ds(Q)=\int_L t_j(Q)u_{ij}^*(Q)\,ds(Q) \tag{17}$$

with

$$\beta_{ij}[u_j(P_1)-u_j(P_2)]=\lim_{\varepsilon\to 0}\int_{L_\varepsilon} t_{ij}^*(Q_\varepsilon)u_j(Q_\varepsilon)\,ds(Q_\varepsilon)$$

where $\beta_{ij}=0$ for $i\neq j$. The curve L_ε is a circle that excludes P_1 and P_2 from the body. Although the auxiliary solutions are also singular at the crack tip P_c, the work integrals along a circle L_ε which encompasses P_c are $0(\varepsilon^{1/2})$ and therefore vanish as ε approaches zero.

Up to this point, only the equations at regular boundary points along a crack have been considered. A similar situation arises at the intersection of the crack with the remaining portion of the boundary. In this case the irregular boundary points at the intersection coincide and, therefore, two additional equations for the translational displacements are needed. Moreover, it is also necessary to introduce an additional equation for the rotations when the intersecting boundaries form two right-angle corners. The equations for the translations can be established using the auxiliary solutions associated with regular points along a crack. However, it is more convenient from a computational standpoint to use

auxiliary solutions that correspond to prying forces acting at the midpoint of a finite crack in an infinite body.

The character of the rotational auxiliary solution is identical to that of the fundamental rotational auxiliary, i.e. $\lambda_n = -1$. However, this solution, unlike the fundamental rotational auxiliary, does not satisfy the local homogeneous boundary conditions [12]. In the crack problem considered in this paper (see Fig. 7), the additional auxiliary is chosen so that the crack remains traction free. In this case, tractions of the order of ρ^{-2} exist along the boundary perpendicular to the crack.

It can be shown that the work integrals with the new kernels are bounded. Exact expressions for these integrals when the interval of integration contains the touching corners are developed in [12].

Non-zero boundary tractions at irregular boundary points

It will be recalled that when the boundary conditions near an irregular point are of the homogeneous type the local displacements can be expressed in terms of an eigenfunction expansion where each of the eigenfunctions conforms to the homogeneous boundary requirements [see equation (8)]. When tractions are applied at an irregular point the actual displacements can be represented by the eigenfunction expansion plus a certain "particular" displacement field which satisfies the nonhomogeneous boundary conditions. For sufficiently smooth loadings, the particular displacements in the vicinity $R^{(p)}$ of an irregular boundary point can be expressed as

$$U_\rho^{(p)} = \sum_n C_n A_n^{(p)}(\phi)\rho^{\lambda_n}$$
$$U_\phi^{(p)} = \sum_n C_n B_n^{(p)}(\phi)\rho^{\lambda_n} \tag{18}$$

where the λ_n are now positive integers. In most practical applications, the boundary tractions vary in some simple fashion in the immediate vicinity of an irregular boundary point, thereby making it possible to obtain the λ_n and C_n by inspection. In more complicated situations where the tractions near the irregular point happen to be nonanalytic, a λ_n representing the non-analytic character of the boundary tractions is chosen. Then the λ_n's associated with the remaining analytic portion of the boundary tractions take on integer values. After the λ_n have been established the C_n can be obtained by an appropriate numerical approximation.

Once the expansion for the particular solution is known, it is a relatively simple matter to include the effects of tractions at irregular points in the formation of the integral equations. The same procedures used in developing equation (15) are used, the only modifications are that the reciprocal work terms contain the particular displacements and tractions enter into the integral equations as known free terms.

NUMERICAL TREATMENT OF BOUNDARY VALUE PROBLEMS

Approximate representation of the integral equations

In most cases exact solutions to the integral equations under consideration are not available. Therefore, one seeks approximate solutions to these equations at discrete boundary points. As an example, consider a region $D+L$ where the boundary points are indicated as shown in Fig. 2.

The appropriate eigenfunction expansions, [11] are used in expressing the boundary values along the intervals extending from the irregular points, up to the so-called transition points (Fig. 2). The boundary values over the remaining intervals are obtained from a parabolic interpolation of the boundary values at the regular boundary points. Since the boundary values at the transition point are expressed entirely in terms of the generalized displacements, the integral equations are written only at the regular and irregular boundary points referred to as ordinary boundary points (see Fig. 2). If the integrals appearing in these equations are approximated by weighted sums, then the set of integral equations can be reduced to a system of linear algebraic equations that involve the generalized displacements and discretized boundary values as unknowns.

Standard quadrature techniques (e.g. trapezoidal rule, Simpson's rule) can be used to approximate the integrals when the integrands are regular. Further refinements can be achieved by subdividing the boundary intervals [12, 13]. In cases where the interval of integration includes a singular point of the kernel the integral is expanded in a series which contains the dominant or singular term. Each term of the series is then integrated exactly. Only a few terms need be retained in most practical computations.

It is important to recognize that local curvature of the boundary can have an important effect on the accuracy of the computation. In order to take this effect into account the boundary curvature along the interval of integration is approximated and enters into the computation [12, 13].

A detailed development of the numerical schemes used in the application of the integral equation method is presented in [12].

The method presented in this paper was used to obtain solutions for the sample problems described in the next section. In these problems it was assumed that the eigenfunction expansions are accurate representations of the actual solution along the intervals that contain the irregular boundary points. The numerical results appear to justify this assumption.

Some numerical results

Numerical solutions for two plane strain problems were obtained in order to test the theory. In each case, the modulus of elasticity was taken as 30×10^6 psi and Poisson's ratio as 0·25. These problems were selected with the aim of investigating both the accuracy and stability of the solutions as affected by:

1. the number and distribution of boundary points; and
2. the number of "modes" in the eigenfunction expansion at irregular boundary points (i.e. the number of generalized displacements to be determined).

One set of solutions was obtained for a notched circular plate (problem 1) subjected to the tractions shown in Fig. 2. The remaining problems set deals with the determination of stresses in a cracked plate. In problem 2, the tractions applied along the boundary are computed from the solution of the Griffith crack problem with the stresses at infinity taken as $\sigma_x = \sigma_y = 30$ ksi and $\tau_{xy} = 0$ (see Fig. 6). The obvious advantage in selecting such a loading is that the numerical results can be compared with the exact solution obtained from the Griffith field.

An exact solution for Problem 1 is not available. However, it is still possible to test whether this solution is consistent by first computing the stresses at specified points near the notch in terms of the eigenfunction expansions for the displacements. Then these stresses can be compared to stresses which are obtained by differentiating the integral

equations for the displacements. In the latter case, the method of determining the stresses begins with the formation of the integral equations (1) for the displacements at the specified points. Then, the integral equations for the strains are obtained by differentiating the kernels underneath the integral sign. That is,

$$\frac{\partial u_j(P)}{\partial x_k} = \alpha_{ij}^{-1}\left[\int_L t_j(Q)\frac{\partial u_{ij}^*(Q)}{\partial x_k}\,ds(Q) - \int_L \frac{\partial t_{ij}^*(Q)}{\partial x_k}u_j(Q)\,ds(Q)\right] \tag{19}$$

where $k = 1, 2$. The values of α_{ij}, of course, depend on whether P is a boundary or interior point. The stresses are easily obtained from the strains in equations (19).

The results presented in the following sections include the displacements at certain boundary points and the stresses at several interior points. Some of the generalized displacements are also tabulated. The units in which the generalized displacements are measured can be deduced from expressions for the displacements [e.g. equations (6)].

(a) *Re-entrant corner problem* (*problem* 1). Solutions for Problem 1 were obtained for a variety of boundary point spacings, some of which are indicated in Figs. 2–4. Displacements and generalized displacements at the 22 ordinary† boundary points in Fig. 2 were

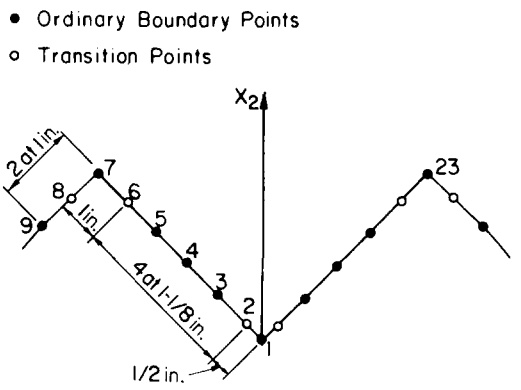

FIG. 3. Boundary points for a notched circular plate.

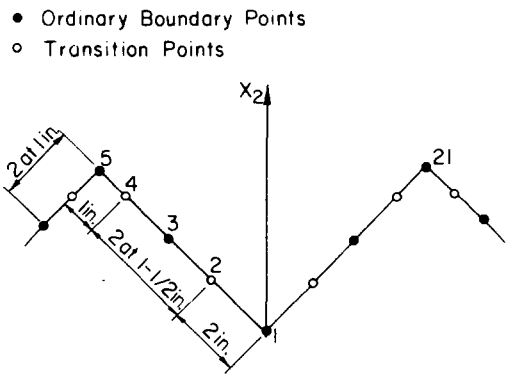

FIG. 4. Boundary points for a notched circular plate.

† At points such as 2 and 28 no equations are written. The field values of these points are determined entirely from quantities defined at the irregular point between them.

obtained using 57 equations. The relative changes in these displacements that result from the choices in the distribution of boundary points indicated in Figs. 3 and 4 are less than 0·5 per cent. As shown in Figs. 3 and 4, the two solutions correspond to 22 and 18 ordinary boundary points, respectively. When 34 ordinary boundary points were used, the relative improvement in the results was approximately 1·5 per cent. This suggests that sufficiently accurate results can be obtained with a fairly small number of equations.

Initially, eleven modes were used in the eigenfunction expansion at the re-entrant corner. The last four terms contribute only a small fraction to the total displacement in the intervals adjacent to the re-entrant corner. The changes in the solution which are observed when the last four modes are omitted are less than 0·1 per cent.

Two different methods were used to compute the stresses $\sigma_\rho, \sigma_\phi, \tau_{\rho\phi}$ at the interior points shown in Fig. 5. Those stresses found by use of the eigenfunction expansions are

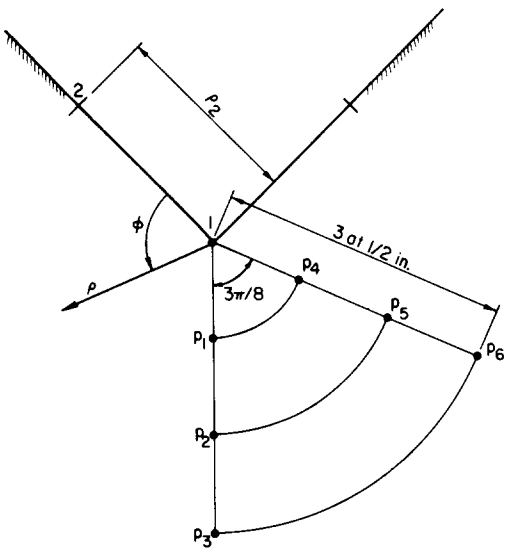

FIG. 5. Location of interior points at which stresses are evaluated.

denoted by $\sigma_\rho^{(1)}, \sigma_\phi^{(1)}, \tau_{\rho\phi}^{(1)}$; the stresses obtained from the integral expressions, equations (19), are denoted by $\sigma_\rho^{(2)}, \sigma_\phi^{(2)}, \tau_{\rho\phi}^{(2)}$. Stress computations were carried out for the boundary point configurations of Figs. 2 and 3, with eleven modes included in the eigenfunction expansion at the re-entrant corner. Approximately 98 per cent of the maximum stresses $\sigma_\rho^{(1)}, \sigma_\phi^{(1)}, \tau_{\rho\phi}^{(1)}$ at the points p_1 and p_4 and 80 per cent at p_3 and p_6 arise from the first nonrigid body mode. This trend is not surprising since this is the only singular symmetric mode in the expansion for the stresses.

It is more significant, however, that the two different methods for computing the stresses give essentially the same results even at the more distant points, p_3 and p_6 where the contribution of the higher modes is not at all negligible (see Table 1).

(b) *The Griffith crack problem* (*Problem* 2). The tractions at a number of boundary points (Fig. 7) were computed from the exact Griffith solution [14]. Approximate displacements at these points were then obtained using the proposed method. The absolute error in these displacements is less than 0·5 per cent. In this case, eight modes with the

TABLE 1. STRESSES NEAR THE RE-ENTRANT CORNER: PROBLEM 1

Interior point	ρ_2† (in.)	$\phi_\rho^{(1)}$ (ksi)	$\sigma_\rho^{(2)}$ (ksi)	$\sigma_\phi^{(1)}$ (ksi)	$\sigma_\phi^{(2)}$ (ksi)	$\tau_{\rho\phi}^{(1)}$ (ksi)	$\tau_{\rho\phi}^{(2)}$ (ksi)
p_1	$\frac{1}{2}$	23·21	23·07	41·77	41·70	0·0	0·0
	1	23·23	23·22	41·79	41·79	0·0	0·0
p_2	$\frac{1}{2}$	13·69	13·60	32·10	32·10	0·0	0·0
	1	13·70	13·69	32·13	32·14	0·0	0·0
p_3	$\frac{1}{2}$	8·96	8·91	28·25	28·26	0·0	0·0
	1	8·97	8·96	28·26	28·29	0·0	0·0
p_4	$\frac{1}{2}$	41·18	40·99	13·67	13·59	18·24	18·30
	1	41·20	41·20	13·68	13·66	18·25	18·26
p_5	$\frac{1}{2}$	31·43	31·33	6·43	6·53	13·90	13·86
	1	31·45	31·43	6·43	6·45	13·91	13·92
p_6	$\frac{1}{2}$	27·48	27·47	2·94	3·02	12·17	12·10
	1	27·49	27·48	2·94	2·99	12·17	12·18

† The length of the intervals adjacent to the irregular point (see Fig. 5).

eigenvalues (λ = 0·0, 0·0, 1·0, 0·5, 1·0, 1·5, 2·0, 2·5)† were used together with the eigenfunction expansions, equations (5), to compute the stresses near the crack tip. It can be seen from Table 2 that the approximate and exact stresses at the interior points in Fig. 7

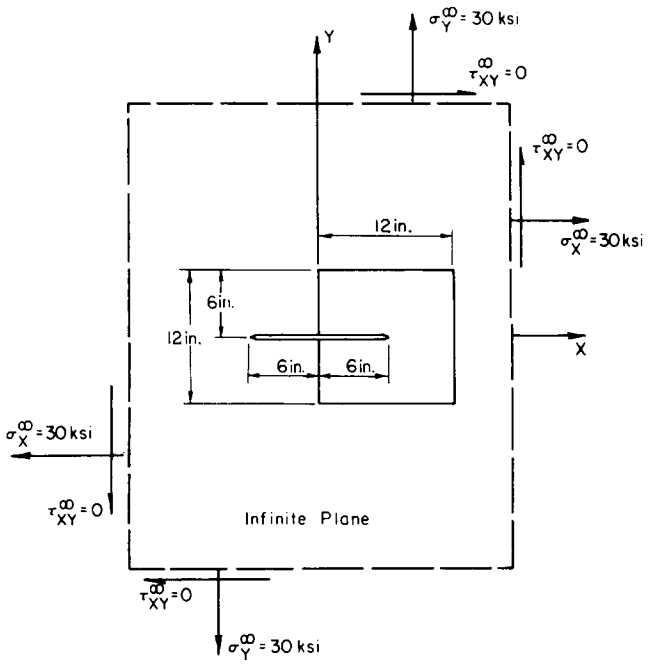

FIG. 6. Data for Problem 2.

† The first three eigenvalues correspond to the rigid-body modes.

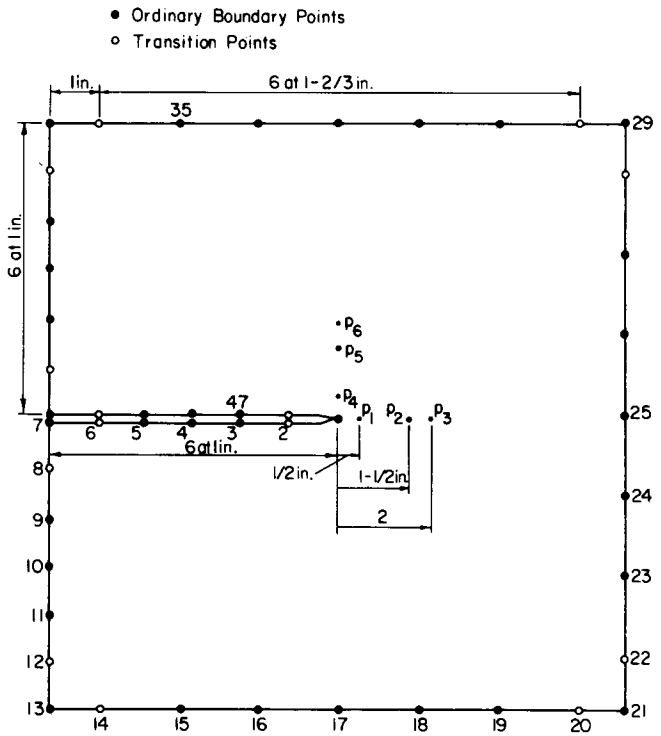

FIG. 7. Boundary and other points for a cracked plate.

agree remarkably well in view of the fact that only 80 algebraic equations at 34 ordinary boundary points were used in obtaining the solution. It is possible to arrive at an accurate estimate of the stresses at sufficiently small distances from the crack tip in terms of just the fourth generalized displacement, which in this case is proportional to the stress intensity factor. The error in the intensity factor was approximately 0·02 per cent.

The stresses at the external corners are computed in terms of the appropriate particular solutions, i.e. equations (18). It should be recalled that these solutions are determined directly from the prescribed boundary tractions near the corners.

TABLE 2. STRESSES NEAR THE TIP OF A CRACK: PROBLEM 2

Interior point	Exact stresses (ksi)			Approximate stresses (ksi)		
	σ_ρ	σ_ϕ	$\tau_{\rho\phi}$	σ_ρ	σ_ϕ	$\tau_{\rho\phi}$
p_1	78·00	78·00	0·0	77·99	77·99	0·0
p_2	50·00	50·00	0·0	49·97	49·97	0·0
p_3	45·36	45·36	0·0	45·29	45·30	0·0
p_4	79·54	30·99	27·52	79·53	31·00	27·50
p_5	47·71	24·07	17·32	47·66	24·18	17·37
p_6	42·09	23·65	15·46	41·99	23·86	15·55

In this problem, it turns out that the crack boundaries are unstrained. It is therefore encouraging that the two generalized displacements which produce stretching along the crack boundaries are negligible when compared to the generalized displacements associated with the opening modes.

The results are stable with respect to changes in the number and distribution of boundary points. For example, errors of less than 2 per cent were observed when 14 of the 34 boundary points in Fig. 7 were removed.

In addition, the results obtained using 34 boundary points remained stable when the number of modes at the crack tip was varied. Errors in the displacements at the ordinary points of approximately 1·0 per cent occurred when the last four modes were omitted from the eigenfunction expansions.

The choice of the length of the intervals adjacent to the crack tip had only a minor effect on the boundary displacements. When eight modes were included at the crack tip and the adjacent intervals in Fig. 7 were doubled to 2 in., errors in the displacements at the boundary points of less than 0·5 per cent were noted.

CONCLUSIONS

The main conclusion that can be drawn from this study is that the extended integral equation method can be applied successfully to a wide range of technically relevant problems. The method is both conceptually simple and numerically effective.

It is clear from the numerical results that the integral equation approach provides accurate solutions that are relatively insensitive to changes in the number and location of boundary points or to the number of eigenfunctions included in the expansion at irregular boundary points. Moreover, these solutions were obtained using a small number of simultaneous equations.

The success of the proposed method is due at least in part to the fact that it leads to a system of linear algebraic equations with large diagonal coefficients, which is one indication of good conditioning. Certain numerical refinements such as subdividing the boundary intervals and including the effect of boundary curvature in the singular integrals also played a particularly important part in achieving accurate results.

An important consideration contributing to the stability of the method is that the generalized displacements cannot couple directly with each other. Rather, they couple with the far-field displacements. This is perhaps the most important reason why the generalized displacements associated with the lower modes were not significantly affected by the addition of the higher modes.

The fact that the generalized displacements depend only on the far-field displacements suggests a simple alternative procedure for estimating the stresses near an irregular boundary point. A finite element analysis which neglects the effect of the nonanalytic perturbations on far-field displacements can be used to determine the far-field displacements. The generalized displacements can then be determined directly from equations (15). This approach will not be as accurate as the proposed method but it can be easily incorporated into existing finite element programs.

Acknowledgements—This work was supported by the Structural Mechanics Program of the Office of Naval Research under Contract N00014-67-A-0305-0010. The material in this paper forms part of a doctoral dissertation by M. R. Barone which was submitted to the Graduate College of the University of Illinois at Urbana-Champaign in partial fulfillment of the requirements for the degree of Doctor of Philosophy in Civil Engineering.

REFERENCES

[1] J. R. RICE, A path independent integral and the approximate analysis of strain concentration by notches and cracks. *J. appl. Mech.* **35**, 374 (1968).
[2] I. N. SNEDDON and M. LOWENGRUB, *Crack Problems in the Classical Theory of Elasticity*. John Wiley (1969).
[3] H. M. WESTERGAARD, Bearing Pressures and Cracks, *Trans. Am. Soc. Mech. Engrs.* **A61**, p. A49 (1939).
[4] F. J. RIZZO, An integral equation approach to boundary value problems of classical elastostatics. *Q. appl. Math.* **25**, 83 (1967).
[5] T. A. CRUSE, Numerical solutions in three dimensional elastostatics. *Int. J. Solids Struct.* **5**, 1259 (1969).
[6] T. A. CRUSE and W. VANBUREN, Three dimensional elastic stress analysis of a fracture specimen with an edge crack. *Int. J. Fracture Mech.* **7**, 1 (1971).
[7] H. F. BUECKNER and I. GIAEVER, The stress concentration of a notched rotor subjected to centrifugal forces. *Z. angew. Math. Mech.* **46**, 265 (1966).
[8] J. TIROSH, A direct method for stress-intensity factor in arbitrary, cracked, elastic bars under torsion and longitudinal shear. *J. appl. Mech.* **37**, 971 (1970).
[9] A. E. H. LOVE, *A Treatise on the Mathematical Theory of Elasticity*, fourth edition. Dover (1944).
[10] M. L. WILLIAMS, Stress singularities resulting from various boundary conditions in angular corners of plates in extension. *J. appl. Mech.* **19**, 526 (1952).
[11] O. K. AKSENTIAN, Singularities of the stress–strain state of a plate in the neighborhood of an edge. *Prikl. Mat. Mekh.* **31**, 193 (1967).
[12] M. R. BARONE, Approximate Determination of Stresses Near Notches and Corners in Elastic Media by an Integral Equation Method, Civil Engineering Studies, SRS 374, University of Illinois (1971).
[13] D. J. FORBES, Numerical Analysis of Elastic Plates and Shallow Shells by an Integral Equation Method, Civil Engineering Studies, SRS 345, University of Illinois (1969).
[14] A. A. GRIFFITH, The phenomena of rupture and flow in solids. *Phil. Trans. R. Soc.* **A221**, 163 (1920).
[15] E. L. INCE, *Ordinary Differential Equations*. Dover (1956).

APPENDIX

Proofs of Propositions 1 *and* 2

Since the mth actual and nth auxiliary solutions appear frequently in the subsequent proofs of propositions 1 and 2 it is convenient to refer to them as:

Solution 1. The mth component of the actual field defined by equations (4)–(8).

Solution 2. The nth auxiliary field defined by equations (9) and (10).

Proof of Proposition 1

Consider the solutions 1 and 2 with $n = m$ and let both solutions be defined in the same annular sector (see Fig. 8). Solution 1 satisfies a set of homogeneous boundary conditions. This fact can be easily confirmed by recalling that λ_m is obtained by expressing the appropriate boundary quantities in terms of Solution 1. This leads to the four linear algebraic equations

$$[a_{ij}(\lambda_m)]_{4,4}[C_{jm}]_{4,1} = [b_{im}]_{4,1}, \text{ for each } m. \tag{A.1}$$

The determinant of this system of equations must be equal to zero in order to insure that a nontrivial solution exists for the homogeneous boundary conditions

$$[b_{im}]_{4,1} = [0].$$

The resulting characteristic equation is then used to determine the admissible values of λ_m. The corresponding boundary values associated with Solution 2 are obtained by replacing λ_m by $-\lambda_m$ in equation (A.1) giving

$$[a_{ij}(-\lambda_m)]_{4,4}[C^*_{jm}]_{4,1} = [b^*_{im}]_{4,1}. \tag{A.2}$$

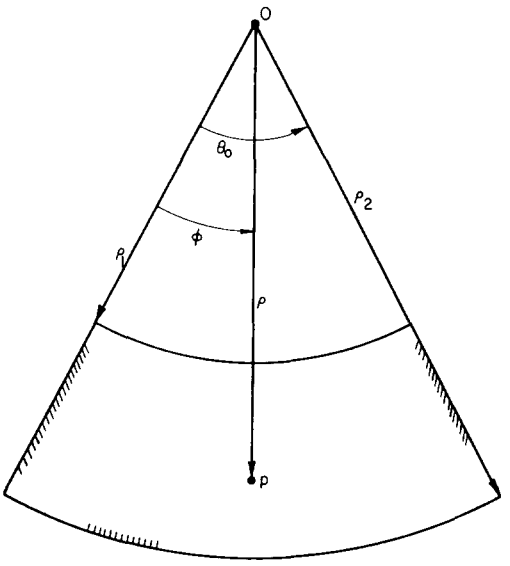

FIG. 8. Annular sector.

If the determinant D^* of this new system vanishes then Solution 2 satisfies the homogeneous boundary conditions and Proposition 1 is proved. Suppose, however, that D^* does not vanish. Then it is always possible to solve for a unique and nontrivial set of $[C^*_{jm}]_{4,1}$ and still satisfy any three of the homogeneous boundary conditions. Now the reciprocal relations are applied using solution 1 and 2 along the boundaries of the annular sector shown in Fig. 8. It is easily seen that the reciprocal work terms along the circular arcs sum to zero. This is apparent from Fig. 8, by noting that the positive directions of tractions are opposite along the two arcs while the positive directions of displacements remain unchanged and that the variation of the stresses and displacements in ϕ is the same along both arcs. Therefore, the reciprocal relations are expressed as

$$\int_{\rho_1}^{\rho_2} [\pi_{12}(\theta_0) - \pi_{12}(0)]\, d\rho = \int_{\rho_1}^{\rho_2} [\pi_{21}(\theta_0) - \pi_{21}(0)]\, d\rho \tag{A.3}$$

where

$$\pi_{12}(\phi) = T_{\phi m} D^*_{\phi m} + T_{\rho\phi m} D^*_{\phi m}, \qquad \pi_{21}(\phi) = T^*_{\phi m} D_{\phi m} + T^*_{\rho\phi m} D_{\phi m}.$$

Since Solution 2 satisfies three of the four homogeneous boundary conditions, all but one of the eight work terms in the reciprocal relation must vanish. But then the remaining term associated with the violated boundary condition must also vanish if equation (A.3) is to be satisfied. The significance of this requirement can be illustrated by considering an example where

$$T_{\rho\phi m}(0) = T_{\rho\phi m}(\theta_0) = T_{\phi m}(0) = T_{\phi m}(\theta_0) = 0.$$

If, in determining Solution 2, $T^*_{\phi m}(0)$ is chosen as the nonzero element of the $[b^*_{im}]_{4,1}$ vector, then the reciprocal relation is given as

$$\int_{\rho_1}^{\rho_2} T^*_{\phi m}(0) D_{\phi m}(0)\, d\rho = 0.$$

Since $T^*_{\phi m}(0)$ is nonzero it follows that $D_{\phi m}(0)$ must be zero. Now the choice of the nonzero element of the $[b^*_{im}]_{4,1}$ vector is completely arbitrary and therefore this analysis can be performed separately for the two independent $[b^*_{im}]_{4,1}$ vectors which violate the two homogeneous boundary conditions on one edge of the annular sector. Clearly, then the assumption that D^* does not vanish necessarily implies that all the nonhomogeneous boundary values of the actual solution vanish along one edge. But if all the tractions and displacements on one edge disappear then the existence and uniqueness theorems for ordinary differential equations [15] applied to equations (3) require that the actual solution vanish everywhere. This, however, is an obvious contradiction, since the actual solution is known to be nontrivial. Hence, D^* must be zero. The extension of this proof to cases other than traction-free wedges is apparent.

Proof of Proposition 2

Consider Solutions 1 and 2 and let them be defined in the same annular sector for any m and n (see Figs. 8 and 9). The reciprocal theorem can be used to relate the two systems

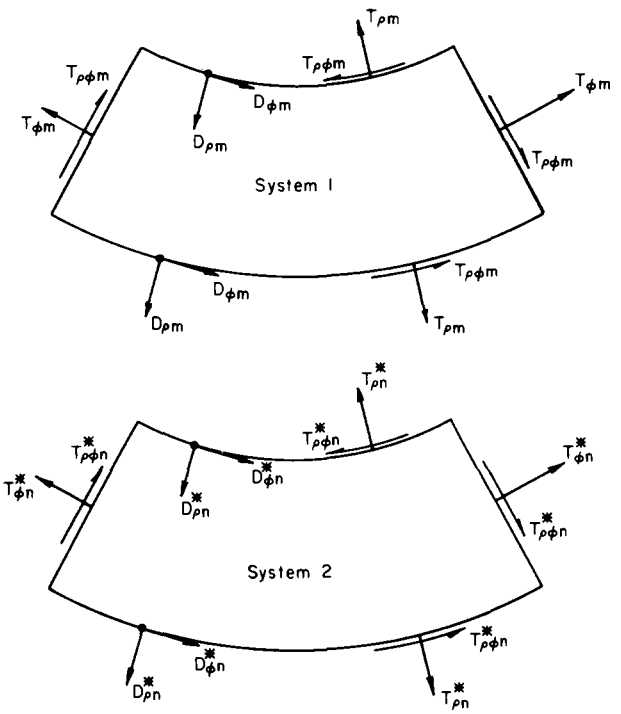

FIG. 9. Systems for developing auxiliary solutions.

of tractions and displacements associated with these two solutions. According to Proposition 1 both of these solutions satisfy the homogeneous boundary conditions.

Consequently, the reciprocal work terms along both radial edges of the annular sector vanish. The remaining reciprocal work terms are related as follows

$$\int_0^{\theta_0} [\Psi_{12}(\rho_1, \phi) - \Psi_{21}(\rho_1, \phi)]\rho_1 \, d\phi = \int_0^{\theta_0} [\Psi_{12}(\rho_2, \phi) - \Psi_{21}(\rho_2, \phi)]\rho_2 \, d\phi \qquad (A.4)$$

where

$$\Psi_{12}(\rho, \phi) = T_{\rho m} D^*_{\rho n} + T_{\rho\phi m} D^*_{\phi n}$$
$$\Psi_{21}(\rho, \phi) = T^*_{\rho n} D_{\rho m} + T^*_{\rho\phi n} D_{\phi m}.$$

Using equations (6), (7), (9) and (10), and letting $\lambda^*_n = -\lambda_n$ it is possible to recast the reciprocal relation as follows

$$\rho_1^{\lambda_m - \lambda_n} \Gamma_{mn} = \rho_2^{\lambda_m - \lambda_n} \Gamma_{mn}. \tag{A.5}$$

where Γ_{mn} is given by equation (13). When m is unequal to n the exponent $\lambda_m - \lambda_n$ is not equal to zero, and since ρ_1 and ρ_2 are arbitrary the reciprocal work equation can be satisfied only if Γ_{mn} is identically equal to zero. If m equals n, equation (A.5) reduces to an identity which reveals no information on the nature of Γ_{nn}.

In the proofs of Propositions 1 and 2 it was assumed that the λ_n were real. However, the proofs remain essentially the same for complex λ_n; the only significant difference is that in this case the reciprocal theorem is applied to complex displacement and stress fields. The generalized force, Γ_{nn}, is derived for complex λ_m in [12].

(*Received* 10 *December* 1971; *revised* 31 *March* 1972)

Абстракт—Дается метод интегрального уравнения, который позволяет опредлить поля напряжений и деформаций вблизи углов и вырезов. Способ расчёта использует хорошо известные выражения асимптотического характера, для полей вблизи искательных точек. Исследуются неизвестные коэффициенты, один из которых является фактором интенсивности напряжений для случая пластинки со щелью, в смысле обощенных перемещений. Разработаны подходяшие опытные решения, с целью представления обобщенных перемещений в форме интегралов, заключающих величины далеких полей. Даются численные решения, полученные из образцов, для пластинок с надрезом и со щелью.